RSC Advances

PAPER

View Article Online
View Journal | View Issue

Cite this: *RSC Adv.*, 2017, **7**, 39244

Novel poly(aniline-*co*-3-amino-4-methoxybenzoic acid) copolymer for the separation and recovery of Pd(II) from the leaching liquor of automotive catalysts

Lijiang Zhong, Jinyan Zhang, Qin Zhang, Muhan Chen and Zhangjie Huang *

Received 8th June 2017
Accepted 5th August 2017

DOI: 10.1039/c7ra06404g

rsc.li/rsc-advances

In this study, novel polyaniline-3-amino-4-methoxybenzoic acid (PANI–AMB) copolymers were prepared and used as adsorbents for the separation and recovery of Pd(II) from a mixed solution containing Pt, Pd, and Rh. Batch sorption studies were carried out, and the main adsorption parameters were systematically investigated. Furthermore, the relevant thermodynamic parameters, isotherms, and kinetic models were also evaluated. Results revealed a high adsorption capacity of 278.5 mg g^{-1} for Pd(II). Separation factors $\beta_{Pd/Pt}$ and $\beta_{Pd/Rh}$ were 4.3 × 10^3 and 5.3 × 10^3, respectively. Results obtained from scanning electron microscopy (SEM), Fourier transform infrared spectroscopy (FT-IR), ultraviolet-visible spectroscopy (UV-vis), X-ray diffraction (XRD), and X-ray photoelectron spectroscopy (XPS) measurements indicated that the sorption of Pd(II) occurs mainly by chelation between Pd(II) and –NH–/–N=/–COOH/–OCH_3 and is accompanied by a redox mechanism involving the reduction of Pd(II) to Pd(0). The new PANI–AMB adsorbent showed efficient adsorption and separation of palladium from the leaching liquor of spent automotive catalysts, as well as good stability and reusability.

1. Introduction

Pt, Pd, and Rh are widely used as automotive catalysts, and together they account for 1000–2000 g t^{-1} of the automotive waste catalysts.[1] However, the content of Pt, Pd, and Rh in the ores of platinum group metals (PGMs) is only 1–10 g t^{-1}.[2] The content of PGMs in automotive waste catalysts is significantly greater than that in their corresponding ores. Hence, in the past few decades, the recycling of Pt, Pd, and Rh from automotive waste catalysts has been an important research area.[3] Nevertheless, the efficient separation of palladium from the leaching liquor of automotive catalysts remains a challenge because its chemical properties are similar to those of other PGMs. Various separation methods including chemical precipitation,[4] solution extraction,[5] membrane separation,[6] reverse osmosis,[7] ion exchange and adsorption have been employed to enrich and separate palladium ions from a mixed solution containing Pt, Pd, and Rh.[3,8] Among these methods, adsorption is the optimum method for removing palladium from leaching solutions containing extremely low concentrations of PGMs. Several sorbents such as activated carbon,[9] biosorbents,[10–12] and functionalized silica[13] have been used to recover palladium. However, a majority of these expensive sorbents exhibit low adsorption capacities, which are not suitable for the separation of palladium ions from the leaching liquor of automotive catalysts. Therefore, it is crucial to develop cost-effective adsorbents, with superior capacities and selectivities, to separate palladium ions for practical applications. In particular, materials exhibiting high adsorption capacities are still lacking, and the preparation of these adsorbents by simple, economic processes is highly anticipated.

In recent years, polyaniline-based adsorbent materials have attracted considerable attention because of their abundant active sites, simple synthesis, excellent stability, and high adsorption capacity. These materials exhibit tremendous potential as cost-effective sorbents for the removal of noble and heavy metal ions, *e.g.*, Ag(I),[14–17] Hg(II),[18–20] Au(III),[21] Pb(II),[22,23] Cr(VI),[24–26] and Cu(II)[27] from aqueous solutions. Compared to the majority of adsorbents reported in the literature, polyaniline-based materials exhibit higher adsorption capacities. For example, Li and co-workers have reported an excellent sorbent for the adsorption of Hg(II), prepared by the classical chemical oxidative copolymerization of aniline and 5-sulfo-2-anisidine. The maximum sorption capacity of this material for Hg(II) was found to exceed 2063 mg g^{-1}, which is possibly the highest capacity reported thus far.[28] The excellent adsorption capacity of polyaniline-based materials is related to the presence of a large number of imino and amino groups linked to the polyaniline chain, which can form complexes with soft metal ions. To date, to the best of our knowledge, there are no studies on the

School of Chemical Science and Technology, Yunnan University, Cuihu North Road No. 2, Kunming 650091, PR China. E-mail: zhjhuang2010@163.com; Fax: +86 871 65036626; Tel: +86 871 65032180

adsorption and separation of Pd(II) from the leaching liquor of automotive catalysts using PANI–AMB copolymer adsorbents. In this study, PANI–AMB copolymers were successfully prepared by oxidative polymerization of aniline with 3-amino-4-methoxybenzoic acid.

According to the hard and soft acid and base (HSAB) theory, N and O atoms are considered as soft Lewis bases, which exhibit strong coordination for Pd(II). Due to the introduction of carboxylic acid and methoxy groups, the PANI–AMB chains contain several N and O atoms, which are beneficial for the adsorption of palladium ions. In addition, Pd(II) can be reduced to Pd(0) by protonated amino (–NH–) and imino (–N=) groups. Therefore, it is expected that the synergistic effects between these functional groups would endow the PANI–AMB copolymers with a high adsorption capacity for palladium(II). Key experimental parameters including optimum HCl concentration, initial Pd(II) concentration, and the maximum adsorption capacity for Pd(II) were investigated. The mechanism of adsorption of Pd(II) onto the PANI–AMB copolymers was studied using SEM, FT-IR, UV-vis, XRD, and XPS analyses. In addition, thermodynamic parameters, isotherms, and kinetic models were systematically investigated.

2. Experimental

2.1 Reagents and instruments

Chemical reagents including aniline (ANI), 3-amino-4-methoxybenzoic acid (AMB), HCl and ammonium persulfate were purchased from Beijing Chemical Reagent Co., Ltd., Beijing, China, and used without further purification. The leaching liquor of automotive catalysts was provided by Yunnan Gold Group Company China. For the preparation of Pd(II) stock solution (10.00 g L^{-1}), palladium powder (2.500 g) was weighed out and transferred into a 400 mL glass beaker. Then, 80 mL of freshly prepared aqua regia (HNO_3 + HCl, 1 : 3 ratio) was added. The beaker was covered with a watch glass and heated on a hot plate. Boiling was continued for at least 4 h and enough aqua regia was added at regular intervals to maintain the free acid level at about one centimeter above the sample level. The watch glass was removed and the content was evaporated slowly until the sample was completely dissolved. Then, 50 mL of 6 mol L^{-1} HCl was added to the beaker and the solution was evaporated to nearly dryness again, and this was repeated 3 times. Then the solution was transferred into a 250 mL volumetric flask, and the final volume was adjusted by adding 0.1 mol L^{-1} HCl solution. Working standard solutions were obtained by appropriate dilution of the stock standard solution.

Molecular weights of the polymers were measured by a gel permeation chromatograph (1515 GPC, Waters Corp., USA) using a column packed with Waters Styragel HT. Nuclear magnetic resonance (NMR) spectra were recorded on a Bruker Avance 400 MHz spectrometer (Bruker, Karlsruhe, Germany) using tetramethylsilane (TMS) as the internal reference. Fourier transform infrared (FT-IR) spectra were recorded on a Thermo NICOLET 8700 spectrometer (USA) in the wavenumber range of 400–4000 cm^{-1}. Ultraviolet-visible (UV-vis) spectra were recorded on a spectrophotometer (UV-2550, Shimadzu Corp., Japan). XRD patterns were obtained to identify the phase structure and composition of the samples over a 2θ range from 10° to 90° using Co Kα radiation. Sample morphologies were observed by scanning electron microscopy (SEM, AMRAY 1000B). Pore volumes and Brunauer–Emmett–Teller (BET) surface areas were measured on a Micromeritics Tristar apparatus (USA) *via* nitrogen adsorption–desorption measurements conducted at 77 K. Thermal properties of the PANI–AMB copolymers were investigated by thermogravimetric analysis (TGA, SDT-Q600, USA) at 25–900 °C under nitrogen. The contents of Pd, Pt, Rh, Fe, Cu, Al, Zn, Pb, and Ni were determined by inductively coupled plasma atomic emission spectroscopy (ICP-AES, ICAP 6300, Thermo Fisher Scientific, Waltham, MA, USA). XPS analysis was performed on a Thermo VG Multilab 2000 spectrometer with a Mg Ka (1253.6 eV) X-ray source and a spherical section analyzer. The pH values were recorded using a PHS-3C precision pH meter (REX Instrument Factory, Shanghai, China).

2.2 Batch adsorption experiments

Batch adsorption studies were carried out to examine the adsorption of Pd(II) on the PANI–AMB copolymers. From the batch experiments, optimum experimental conditions, kinetics, and thermodynamics were investigated. In a typical experiment, the PANI–AMB copolymer (50 mg) was dispersed in a Pd(II) solution (20 mL). After 45 min, the solution was subjected to centrifugation for 5 min at 3000 rpm. The initial and final concentrations of the metal ions in solution were measured by ICP–AES. Efficiency of adsorption (E_M, %) and the equilibrium adsorption capacity (q_e, mg g^{-1}) were calculated according to the following equations:

$$E_M = \frac{C_0 - C_e}{C_0} \times 100\% \quad (1)$$

$$q_e = \frac{(C_0 - C_e) \times V}{W} \quad (2)$$

where C_0 (mg L^{-1}) is the initial concentration of metal ions, C_e (mg L^{-1}) is the equilibrium concentration of metal ions, W is the mass of adsorbent added (g), and V is the volume of the solution of metal ions.

3. Results and discussion

3.1 Molecular weight determination and ^{1}H-NMR spectroscopy

Polyaniline-3-amino-4-methoxybenzoic acid (PANI–AMB) copolymers were synthesized according to Scheme 1.[29]

A typical synthesis procedure of PANI–AMB copolymers is as follows: Aniline (2.33 g, 25 mmol) and AMB (4.18 g, 25 mmol) were dissolved in 150 mL of a 1 mol L^{-1} HCl solution. Then, ammonium persulfate (11.4 g, 50 mmol) was mixed with 50 mL of a 1 mol L^{-1} HCl solution to prepare an oxidant solution. Next, the oxidant solution was added into the mixed solution of ANI and AMB. The reaction mixture was then continuously stirred for 24 h at room temperature. The product was collected by centrifugation and washed with absolute ethanol. Finally, the resulting dark green powder was dried in a vacuum oven at

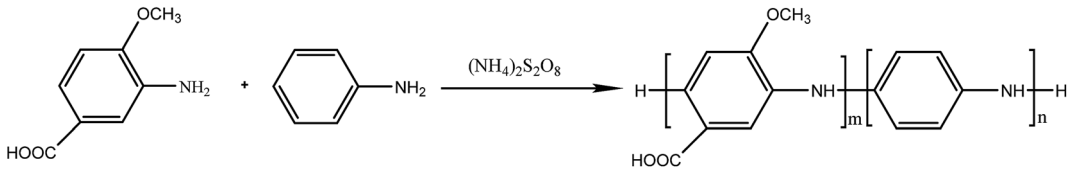

Scheme 1 Synthesis of PANI–AMB copolymers.

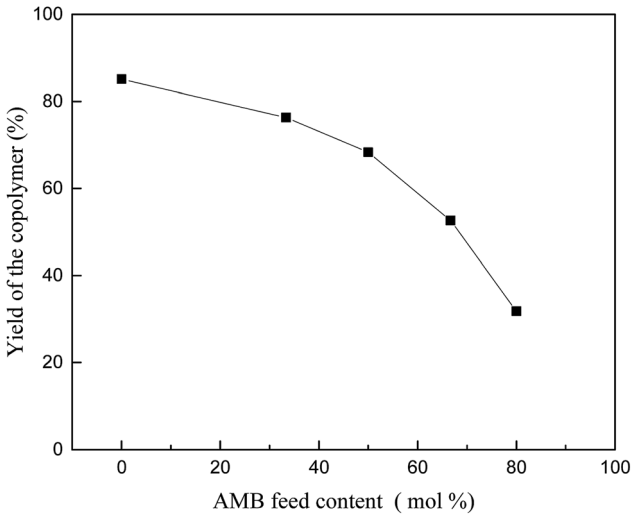

Fig. 1 Yield of the copolymers in different AMB feed content.

40 °C for 48 h. A 68.3% yield was obtained for poly (aniline-*co*-3-amino-4-methoxybenzoic acid). PANI–AMB copolymers with different the AMB/ANI feed ratios were synthesized by the same method. Five different the AMB/ANI feed ratios were used to investigate their effects on the yield of PANI–AMB copolymers. Fig. 1 indicated that yield of PANI–AMB copolymers strongly depends on the AMB/ANI feed ratios. By increasing the AMB feed content from 0 to 80 mol%, the yield of the copolymers decreased from 85.1 to 31.8%. The main reason was that hydrophilic carboxylic acid groups in AMB unit can enhance the water solubility of PANI–AMB copolymers.[28,29]

The solubility of PANI–AMB in THF is very low, and PANI–AMB can be completely dissolved in DMF without leaving any residue in solution. Molecular weights of PANI–AMB copolymers were measured by a gel permeation chromatograph (GPC) using a column packed with Waters Styragel HT, which was eluted by DMF at a flow rate of 1.0 mL min^{-1}. The molecular weights of PANI–AMB copolymers dissolved in DMF was measured by GPC, and the results are listed in Table 1.

The ^{1}H-NMR spectra of PANI–AMB copolymers exhibited peaks at 3.91 ppm which are associated with OCH_3 groups. The peak at 5.59 ppm is assigned to NH groups,[30] Those peaks between 6.97 and 8.02 ppm can be ascribed to hydrogens of benzene ring,[31] and the peak at 8.90 ppm is due to COOH groups. The ^{1}H-NMR spectra of PANI–AMB is shown in Fig. 2.

Table 1 Molecular weight of PANI–AMB copolymers determined by GPC

Copolymer	Solvent	M_n	M_w	M_p	M_z	M_w/M_n
PANI–AMB	DMF	13 825	16 517	16 166	19 904	1.19

3.2 Thermal stability of PANI–AMB copolymers

The thermal stability of the materials was evaluated by TGA under N_2 (Fig. 3).

Samples were heated from 25 to 900 °C. A three-step weight loss was observed in the TGA curve of the PANI–AMB copolymers. The first weight loss was up to 5% and occurred at 25–90 °C, corresponding to the removal of intramolecular solvents. The second weight loss of 10% was observed at around 200 °C, corresponding to the thermal decomposition of the residual organic matter. The third weight loss of 40.1% was observed at 200–500 °C due to the partial collapse of the polymer. Above 500 °C, the resin dissociated into various low-molecular-weight products. After heating to 900 °C, the residual mass percentage of the resin was less than 35.0%. The PANI–AMB copolymers

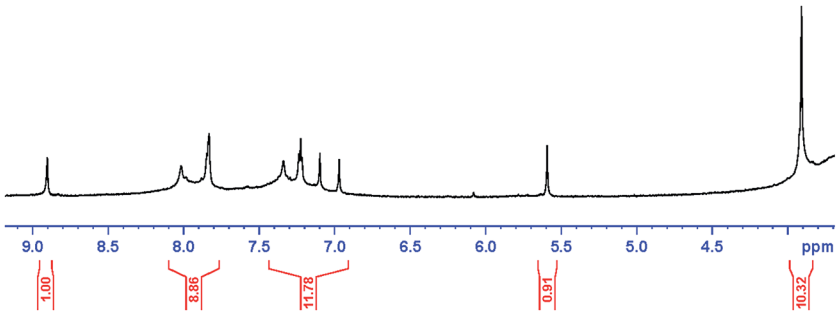

Fig. 2 ^{1}H-NMR spectra of PANI–AMB copolymers.

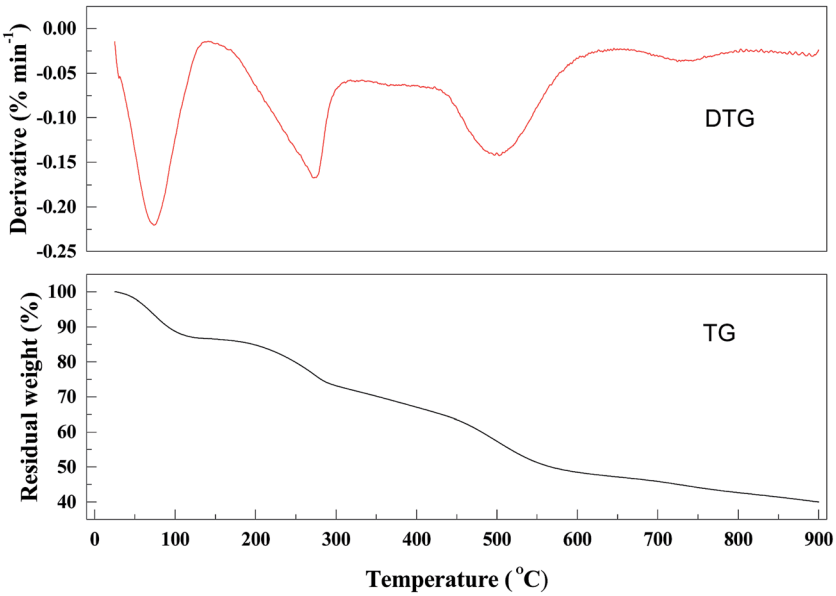

Fig. 3 TG-DTG curves of PANI–AMB copolymers.

exhibited similar thermal stability as some other polyaniline-based sorbents based on the reported TGA curves (Table 2).

3.3 Optimization of the ANI/AMB ratio

PANI–AMB copolymers with different AMB/ANI molar ratios were synthesized by traditional chemical oxidative polymerization. Five different AMB : ANI molar ratios were used to investigate their effects on the Pd(II) sorption of PANI– AMB copolymers (Fig. 4). The results indicated that AMB feed content remarkably affected the adsorption capacity of copolymers. AMB unit in the polymer played a significant role in the adsorptivity of Pd(II). By increasing the AMB feed content from 0 to 50 mol%, adsorption capacities of the copolymers for Pd(II) increased from 135.4 to 148.0 mg g^{-1}. The main reason was that $-OCH_3$ and –COOH groups of AMB unit in the polymer exhibit good chelation with palladium ions. When the AMB feed content was 50 mol%, the PANI–AMB copolymers showed maximum adsorption capacity. On the other hand, as the AMB feed content increased from 50 to 80%, the corresponding PANI–AMB copolymers exhibited gradually enhanced solubility in the solution. Therefore, the copolymer particles with an AMB feed content of more than 50 mol% are not suitable as sorbents because they are not very stable in dilute acidic media. Similar results have been reported by Li *et al.* for Ag(I) removal with AN/SA.[17] Hence, the PANI–AMB copolymers for adsorption of Pd(II) were prepared with a fixed AMB : ANI molar ratio of 50 : 50 for the following study.

Table 2 Comparison of the thermal stability with other polyaniline-based sorbents

Adsorbent	Peaks at the DTG curve (°C)	Ref.
AN/SA	92, 203, 572	17
PANI–LS	102, 270, 496	32
PANI–AMB	85, 275, 550	Present work

3.4 Effect of hydrochloric acid concentration

It is known that, when hydrochloric acid concentration in the aqueous phase is lower than 0.001 mol L^{-1}, the primary Pd(II) species are $Pd(OH)^+$, $Pd(OH)_2$, or $Pd(OH)_4^{2-}$.[33] Hence, in order to find an optimum HCl concentration for selective adsorption of Pd(II), the HCl concentration was varied from 0.01–4.0 mol L^{-1}. Fig. 5 shows the results for single Pd(II) solution experiments. In single Pd(II) solution experiments, the following experimental parameters were fixed constant: initial Pd(II) concentration, 389.0 mg L^{-1}; solution volume, 20.0 mL; amount of PANI–AMB copolymer, 50 mg; temperature, 298 ± 1 K; and adsorption time, 45 min. The adsorption capacity of

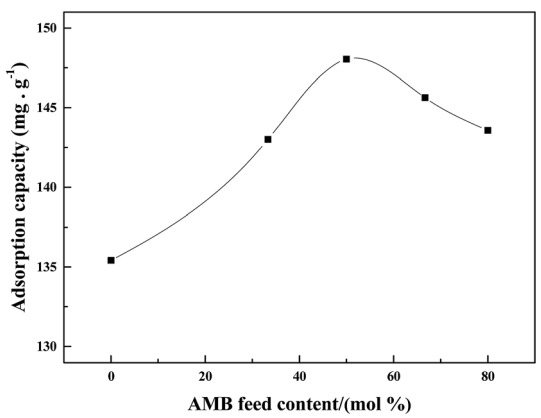

Fig. 4 Adsorption capacity of the copolymers in different AMB feed contents. (Initial Pd(II) concentration of 442.0 mg L^{-1}, T = 298 K, t = 45 min).

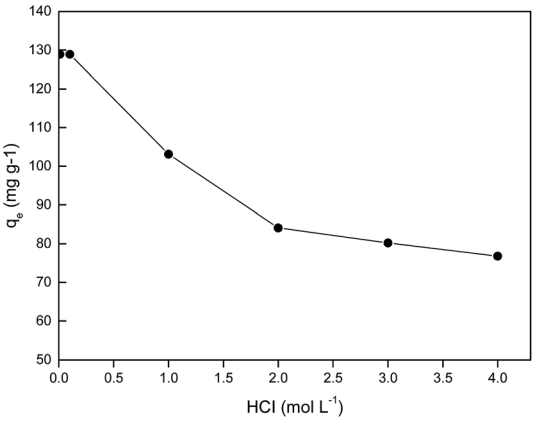

Fig. 5 Effect of HCl concentration on adsorption capacity of the copolymer for Pd(II).

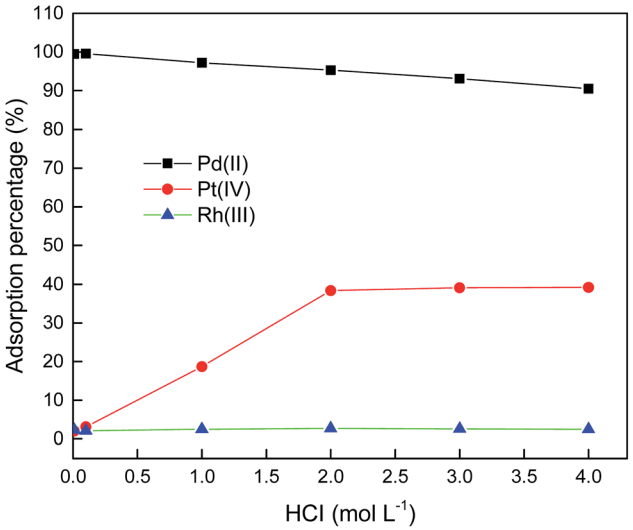

Fig. 6 Effect of HCl concentration on the selective adsorption of Pd(II) over Pt(VI) and Rh(III).

the PANI–AMB copolymer for Pd(II) was almost constant (128.9 mg g^{-1}) with the increase in HCl concentration of aqueous-phase from 0.01 to 0.1 mol L^{-1}. With the further increase in aqueous-phase HCl concentration from 0.1 to 4.0 mol L^{-1}, the adsorption capacity of the PANI–AMB copolymer decreased from 128.9 mg g^{-1} to 76.8 mg g^{-1}. The maximum adsorption capacity for Pd(II) was achieved using an aqueous-phase HCl concentration from 0.01 to 0.1 mol L^{-1}, which is possibly related to the competitive adsorption of Pd(II) and H^+.[15] Furthermore, with increasing HCl concentration, the ratio of the protonated amino and imino groups increased, resulting in less binding sites available for coordination with palladium.[34] Similar results have been reported by Zhai *et al.* for Hg(II) removal with polyaniline/attapulgite composite.[18]

Adsorption experiments were also performed using synthetic solutions containing mixtures of Pd(II), Pt(IV), and Rh(III) with PANI–AMB copolymers as adsorbent. In these experiments, the conditions were: Pd(II), Pt(IV), and Rh(III) concentrations of 250, 200 and 150 mg L^{-1}, respectively; solution volume, 50.0 mL; amount of PANI–AMB copolymer, 200 mg; temperature, 298 ± 1 K; and adsorption time, 45 min. The results of these adsorption selectivity experiments are shown in Fig. 6. The adsorption of Pd(II) over Pt(IV) and Rh(III) from the combined solution was similar to that from single Pd(II) solution at the same HCl concentration. Adsorption percentage of Pd(II) decreased with increasing HCl concentration. Thus, HCl concentration significantly affected the separation of Pd(II) from Pt(VI) and Rh(III). Adsorption percentage of Rh(III) was lower than 3.0% at all HCl concentrations in our experimental range. The adsorption percentage of Pt(IV) also depended on the concentration of HCl. When HCl concentration was 0.1 mol L^{-1}, adsorption percentage of Pt(IV) was 3.1%. Adsorption percentage of Pt increased with increase in HCl concentration up to 2.0 mol L^{-1} and then remained almost constant.

When Pd(II), Pt(IV), or Rh(III) is adsorbed on PANI–AMB copolymers, chloride ions bound to $PdCl_4^{2-}$, $PtCl_6^{2-}$, or $RhCl_6^{3-}$ may be released from the complex. The charge difference between the metal center and chlorine ligands of $PdCl_4^{2-}$ is the smallest among the three platinum group metals.[35] Hence, the preferential adsorption of Pd(II) over Pt(IV) and Rh(III) by PANI–AMB can be explained by the fact that the release of chloride ligands from $PdCl_4^{2-}$ complex is easier than that from $PtCl_6^{2-}$ or $RhCl_6^{3-}$ complexes.

Furthermore, $PtCl_6^{2-}$ was adsorbed on PANI–AMB copolymers through an ion-association mechanism. With increasing HCl concentration, the N and O atoms on PANI–AMB surface were protonated. Thus, the adsorbent surface exhibited positive charges, which enhanced its ion-association ability with $PtCl_6^{2-}$. Therefore, adsorption percentage of Pt(IV) increased with increase in HCl concentration. Similar results have been reported by Lee *et al.*[36]

The charge density of $PtCl_6^{2-}$ (38.2) is smaller than that of $RhCl_6^{3-}$ (54.2).[35] According to the principle of minimum charge density, species with low charge density can be paired more easily than species with higher charge density. $PtCl_6^{2-}$ tends to combine with fewer water molecules to constitute a smaller hydration shell, which is favorable for ion-pair formation.[37–40] Therefore, the adsorption percentage of $RhCl_6^{3-}$ would be lower than that of $PtCl_6^{2-}$.

These results indicate that control of HCl concentration is very important to preferentially separate Pd(II) from Pt(IV) and Rh(III) by PANI–AMB copolymers. When HCl concentration of the aqueous phase was in range of 0.01 to 0.1 mol L^{-1}, Pd(II) could be selectively adsorbed from the mixed solution containing Pd(II), Pt(IV) and Rh(III). For practical applications, 0.1 mol L^{-1} HCl is convenient. Therefore, in the following Pd(II) separation study, HCl concentration of the aqueous phase was maintained at 0.1 mol L^{-1}.

3.5 Effect of the initial palladium ion concentration

With increase in the initial palladium ion concentration, the adsorption capacity increased, while the adsorption rate decreased (Fig. 7). The highest adsorption capacity was 276.2 mg g^{-1} at a palladium ion concentration of 2500 mg L^{-1}.

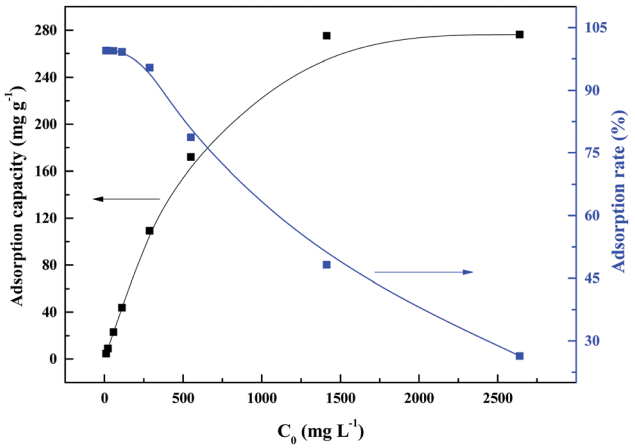

Fig. 7 Effect of initial palladium ion concentration on sorption of PANI–AMB copolymer at 298 K for 45 min.

Above this concentration, no significant changes in the adsorption capacity were observed.

Table 3 summarizes the maximum adsorption capacities and the optimum experimental conditions of previously reported adsorbents for Pd(II). The adsorption capacity of the PANI–AMB copolymer was greater than those of the reported adsorbents, indicating the better performance of PANI–AMB copolymer for the adsorption of Pd(II).

3.6 Sorption kinetics and isotherms

In this study, the pseudo-first-order, pseudo-second-order, and intraparticle diffusion kinetic models[1,48] were employed to test the fitting of experimental data for the adsorption of Pd(II) on the PANI–AMB copolymers. Table 4 and Fig. 8 show the results obtained.

The pseudo-second order model fitted the experimental data better than the pseudo-first-order and intraparticle diffusion models according to their corresponding correlation coefficients R^2 (Table 4 and Fig. 8). Hence, it is evident that chemical sorption is the rate-controlling step.[17]

In this study, the sorption of palladium ions was further described using the Langmuir and Freundlich models (Table 5 and Fig. 9).[49]

The Langmuir isotherm model clearly exhibited the best correlation for the adsorption of Pd(II) on the PANI–AMB copolymer. The theoretical maximum sorption capacity (Q_m) obtained from the Langmuir isotherm model was 278.5 mg g^{-1}. This value is in good agreement with the experimental maximum adsorption capacity of 276.2 mg g^{-1}.

To thoroughly investigate the adsorption of Pd(II) on the PANI–AMB copolymers, relevant thermodynamic parameters for adsorption were also calculated. Specifically, the Gibbs free energy changes (ΔG), entropy changes (ΔS), and enthalpy changes (ΔH) were calculated using the following equations:[50]

$$K_c = \frac{q_e}{C_e} \quad (3)$$

$$\ln K_c = -\frac{\Delta H}{RT} + \frac{\Delta S}{R} \quad (4)$$

$$\Delta G = \Delta H - T\Delta S \quad (5)$$

here, K_c is the thermodynamic equilibrium constant, and q_e and C_e are the equilibrium adsorption capacity and equilibrium concentration of the palladium solution (mol L^{-1}), respectively.

Table 3 Comparison of the optimum experimental conditions and the maximum adsorption capacity for Pd(II) with other adsorbents

Used materials	The optimum experimental conditions (pH, time, sorbent dosage)	Maximum sorption capacity (mg g^{-1})	Ref.
Mesoporous adsorbent	pH = 2, t = 25 min, dosage: 0.5 g L^{-1}	191.35	41
IXAD-7	pH = 4, t = 3 h, dosage: 3.3 g L^{-1}	134.7	1
MP-102	pH = 2, t = 1000 min, dosage: 0.6 g L^{-1}	107.5	42
Chitosan	pH = 3,t = 3 h, dosage: 15 g L^{-1}	19.26	10
Pyrogallol resin	pH = 4, t = 60 min, dosage: 0.4 g L^{-1}	114.3	43
Amberlite XAD resin	pH = 4, t = 60 min, dosage: 3.3 g L^{-1}	50.0	44
Algal beads	pH = 2.5, t = 72 h, dosage: 2 g L^{-1}	136.2	45
Cellulose–MBT	pH = 5.0, t = 3 h, dosage: 20 g L^{-1}	5.00	46
Functionalized nanofibers	1 M HCl, t = 30 min, dosage: 50 g L^{-1}	4.3	47
PANI–AMB copolymer	0.1 M HCl, t = 45 min, dosage: 2.5 g L^{-1}	278.5	Present work

Table 4 Kinetic parameters of Pd(II) adsorption onto the PANI–AMB copolymers

Pseudo-first-order model		Pseudo-second-order model		Intra-particle diffusion model	
$q_{e,exp.}$ (mg g^{-1})	177.7	$q_{e,exp.}$ (mg g^{-1})	177.7	K_p (mg g^{-1} $min^{-0.5}$)	9.622
$q_{e,cal.}$ (mg g^{-1})	58.14	$q_{e,cal.}$ (mg g^{-1})	185.5	C	121.5
k_1 (min^{-1})	0.07	k_2 (g mg^{-1} min^{-1})	0.036	R^2	0.8168
R^2	0.9341	R^2	0.9988		

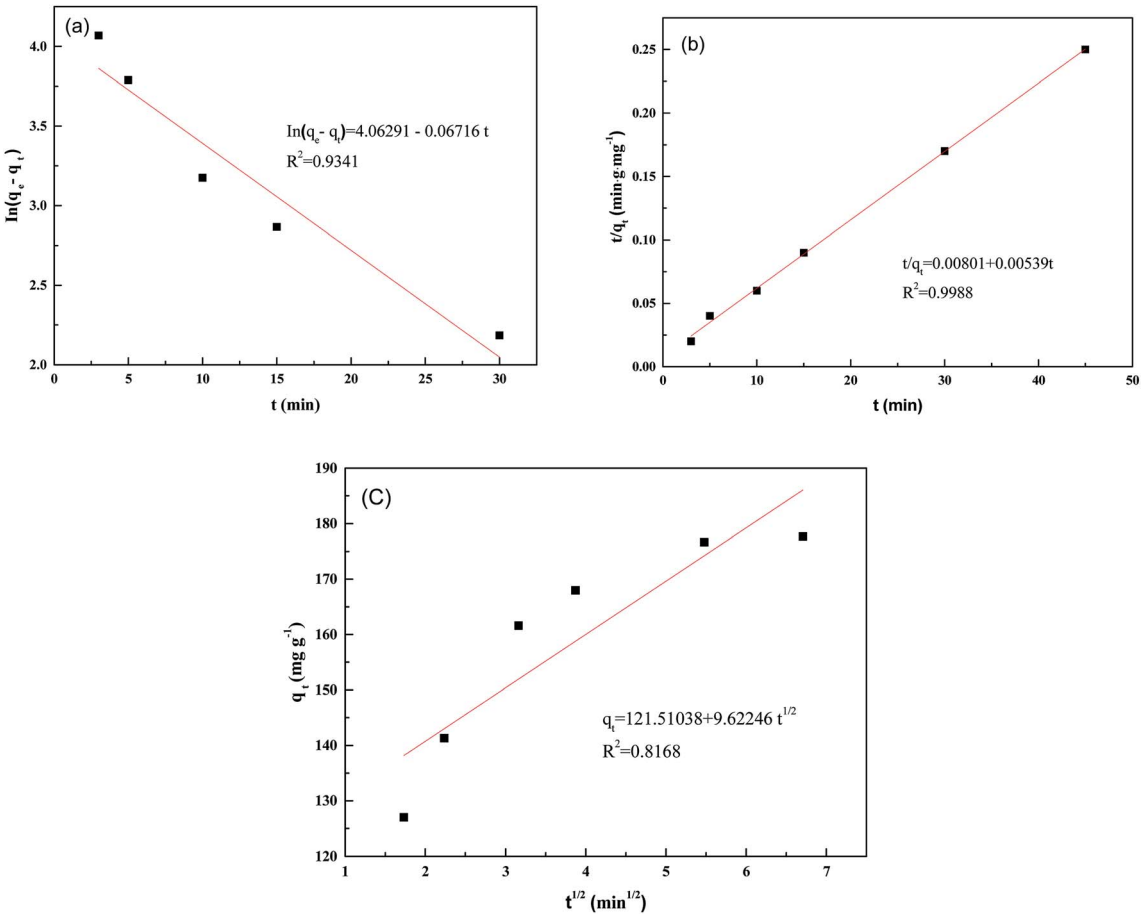

Fig. 8 Pseudo-first-order (a), pseudo-second-order (b), and intra-particle diffusion model (c) at 298 K.

Table 5 Langmuir and Freundlich isotherm parameters of PANI–AMB copolymer

	Langmuir isotherm			Freundlich isotherm		
$q_{m,exp.}$ (mg g^{-1})	$q_{m,cal.}$ (mg g^{-1})	b (L mg^{-1})	R^2	K_f (L g^{-1})	n	R^2
276.2	278.5	0.059	0.9989	25.48	2.67	0.9198

By plotting lnKc *versus* T^{-1}, ΔH and ΔS values were calculated from the slope of the straight line and intercept, respectively. The ΔG values were calculated according to eqn (5), and the results are shown in Table 6. The ΔG values were −16.5, −18.6, −20.7, and −22.6 kJ mol^{-1} at 298, 308, 318, and 328 K, respectively, indicative of a spontaneous reaction (Table 6). Moreover, the degree of spontaneity of adsorption increased with increasing temperatures. Hence, the increase in temperature is favorable for adsorption. A positive ΔH (43.0 kJ mol^{-1}) value confirmed that the reaction is endothermic, while a positive ΔS value indicated that increased randomness is observed at the interface between PANI–AMB and the solution during the adsorption of palladium on PANI–AMB copolymers.[1] If the temperature is sufficiently high, $T\Delta S$ would be greater than ΔH ($\Delta G < 0$). The ΔG values decreased with increasing temperatures (Table 6), indicating that adsorption is more spontaneous at high temperatures. Shen *et al.*[51] have suggested that the ΔH for chemisorption is greater than 40 kJ mol^{-1}. Thus, the ΔH value in Table 6 indicated that chemisorption is possibly the rate-controlling step for the adsorption of Pd(II) on PANI–AMB copolymers.

3.7 Adsorption mechanism and characterization of adsorbents

The initial stage of adsorption involves chelation adsorption predominantly occurring between neutral amine or imine, methoxy and carboxyl groups with Pd(II). Because of its strong basic properties, PANI–AMB can be easily protonated by the acid in the solution. Imine (–N=) atoms in the PANI–AMB chain can be preferentially protonated. The protonated imine groups participate in the redox sorption of Pd(II). As a result of sorption, –NH– and $–NH^+=$ are oxidized to form –N= groups.

SEM, nitrogen adsorption–desorption measurements, FTIR, UV-vis, XRD, and XPS spectra were used to characterize the

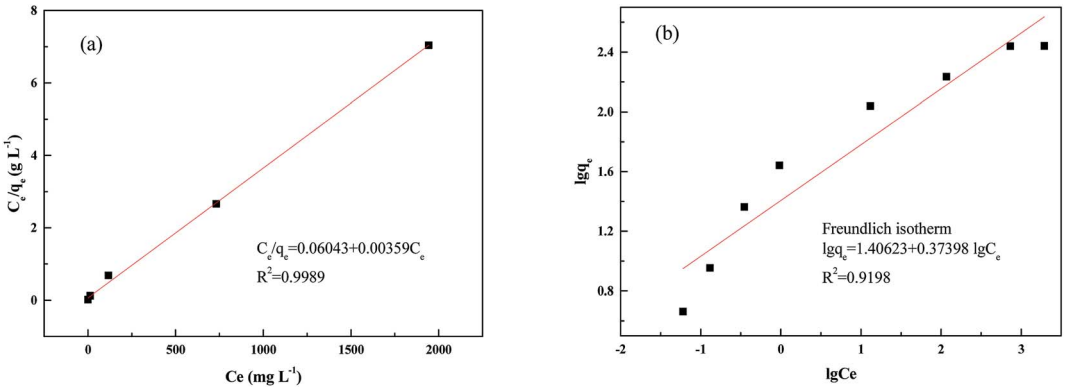

Fig. 9 Langmuir (a) and Freundlich (b) isotherm models.

Table 6 Thermodynamic parameters for the absorption of Pd(II)

Temperature (K)	ΔG (kJ mol^{-1})	ΔS (J mol^{-1} K^{-1})	ΔH (kJ mol^{-1})
298	−16.5	199.9	43.0
308	−18.6		
318	−20.7		
328	−22.6		

adsorbents and confirm the interactions between the adsorbents and palladium ions. Fig. 10 shows the SEM image of the Pd-adsorbed PANI–AMB copolymer particles and the corresponding EDS spectrum. The PANI–AMB copolymer surface exhibited a loose porous structure (Fig. 10a), which contributed to the enhanced adsorption performance. Dark and bright areas were distinguished on the Pd-adsorbed PANI–AMB surface (Fig. 10b). The bright areas were enriched with the Pd complex,

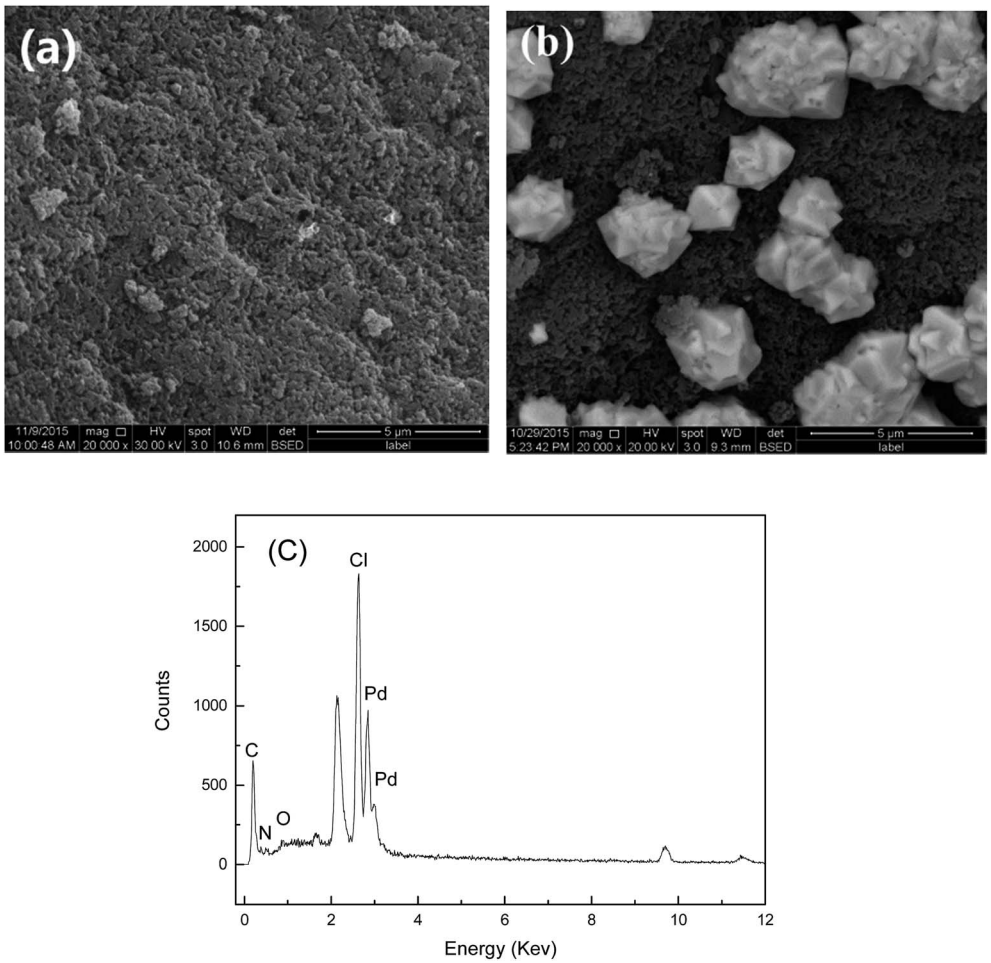

Fig. 10 SEM images of PANI–AMB (a), PANI–AMB-Pd (b), EDS curves of PANI–AMB-Pd sample (c).

indicative of the coordination of the PANI–AMB copolymers with palladium ions.[52] The EDS spectrum of Pd-adsorbed PANI–AMB confirmed the presence of C, O, Pd, N, and Cl on the copolymer surface (Fig. 10c). From the SEM and EDS results, it is evident that the palladium chloro complexes are adsorbed on the PANI–AMB copolymer surface, and some new complexes are formed between $PdCl_4^{2-}$ and sorbents.

Fig. 11 shows the N_2 adsorption–desorption isotherms and the corresponding pore size distribution of the PANI–AMB copolymer. A type IV isotherm was observed, which is characteristic of mesoporous materials. The pore size distribution of the samples was calculated by the Barrett–Joyner–Halenda model. The mean pore diameter, total pore volume, and BET surface area of the PANI–AMB copolymer were 22.67 nm, 0.283 $cm^3\ g^{-1}$, and 49.88 $m^2\ g^{-1}$, respectively. A large total pore volume indicates that the PANI–AMB copolymer has a loose mesoporous structure, which contributes to the enhanced adsorption performance.

Fig. 12 shows the FT-IR spectra of PANI–AMB and Pd-adsorbed PANI–AMB. In the spectra of PANI–AMB, peaks were observed at 1571 and 1492 cm^{-1}, corresponding to the characteristic stretching vibrations of quinoid and benzenoid rings, respectively. Peaks observed at 1302 and 1243 cm^{-1} corresponded to the C=N stretching vibration of the quinoid ring and the C–N stretching vibration of the benzenoid ring, respectively.[28] After the adsorption of Pd(II), the intensity of the peak at 1302 cm^{-1} became stronger, implying that C–NH– in the polymer chains is partly oxidized into C=N. Furthermore, the intensity ratio of the two absorption bands at ~1571 and 1492 cm^{-1} (I_{1571}/I_{1492}) is indicative of the extent of oxidation of the polymer, which reflects the relative content of the quinoid diimine and benzene ring structures.[53] From Fig. 12, the I_{1571}/I_{1492} values after the sorption of Pd(II) were greater than those before the sorption of Pd(II), indicating that a high number of benzenoid rings are oxidized into quinoid rings during sorption. A peak was observed at 1138 cm^{-1}, corresponding to the C–H

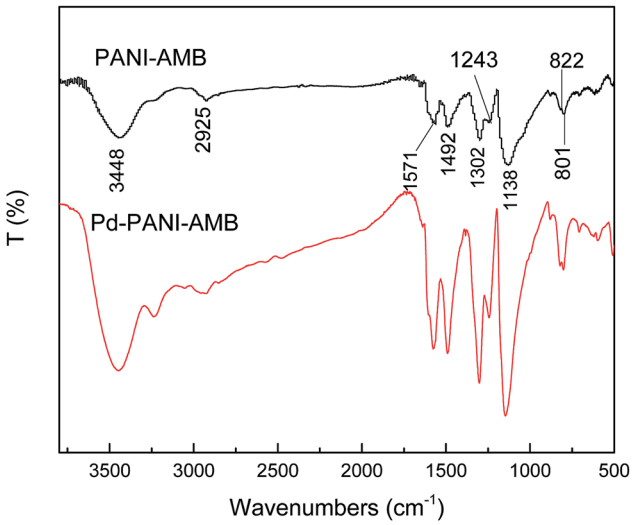

Fig. 12 FT-IR spectra of PANI–AMB, and PANI–AMB-Pd.

aromatic in-plane bending, which is related to the doped structure. Peaks observed at 822 and 801 cm^{-1} corresponding to the 1,2,4,5-tetrasubstituted benzenoid rings of the AMB units barely changed before and after the adsorption of Pd(II), indicating that AMB units are not oxidized by Pd(II).[28] FTIR spectra revealed that the PANI units of the PANI–AMB copolymer are oxidized by Pd(II), thus confirming that redox reaction between PANI–AMB and palladium ions occurs during sorption.

Fig. 13 shows the UV-vis absorption spectra of the copolymers. Absorption peaks were observed at 321 and 585 nm for PANI–AMB, corresponding to the π–π* transition of the benzenoid ring and the n–π* excitation of benzenoid to the quinoid ring in the polymer chain, respectively. After the adsorption of Pd(II), the n–π* band was red-shifted to 620 nm, indicating that a large number of –NH– groups are transformed into –N= groups, and the polymer conjugation length increases.[17] This result is in agreement with the IR results. The UV-vis and IR spectral results support the redox sorption

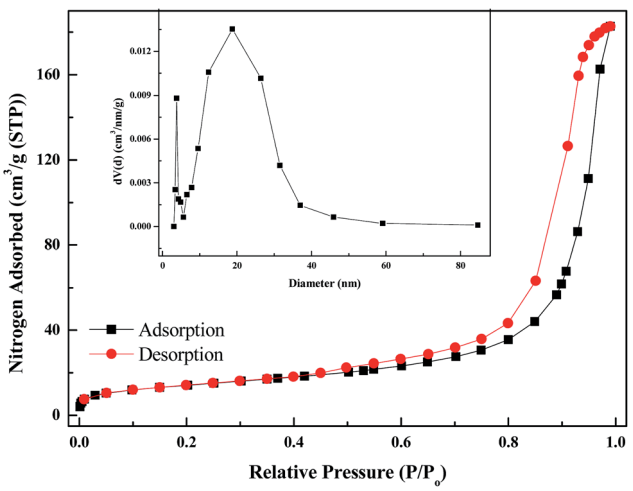

Fig. 11 Nitrogen adsorption–desorption isotherm and Barrett–Joyner–Halenda (BJH) pore size distribution plot (inset) of the PANI–AMB copolymer.

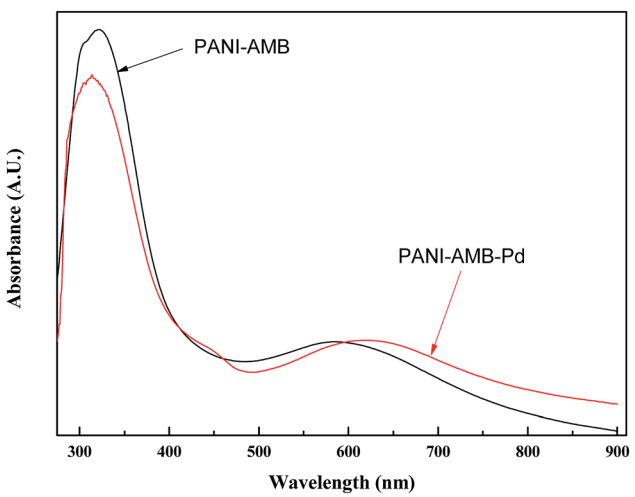

Fig. 13 UV-vis spectra of PANI–AMB, and PANI–AMB-Pd.

mechanism of Pd(II) on the PANI–AMB copolymer. The UV-vis absorption spectra further verify that some of the –NH– groups are oxidized into –N═ groups with the progress of sorption. This finding is in agreement with that obtained from the FT-IR spectra.

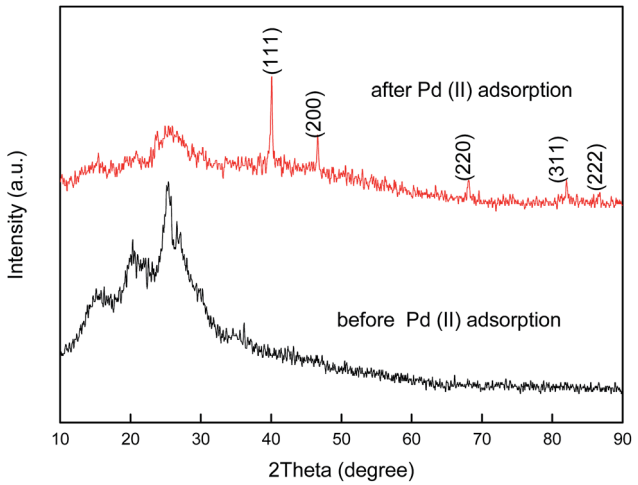

Fig. 14 XRD spectra of PANI–AMB copolymers before and after Pd(II) adsorption.

To provide further evidence for the redox adsorption mechanism, the XRD patterns of PANI–AMB and palladium-adsorbed PANI–AMB were recorded, as shown in Fig. 14. The XRD pattern of PANI–AMB before the adsorption of Pd(II) only exhibited a broad band at around 27°, corresponding to the amorphous phase of PANI–AMB. However, after the adsorption of palladium, peaks were observed at 2θ = 40.01, 46.53, 67.92, 81.85, and 86.34°, corresponding to the (111), (200), (220), (311), and (222) reflections of Pd.[43] This result is in agreement with the XRD pattern of palladium (PDF Card#88-2335).

To confirm the formation of the Pd–N and Pd–O bonds in the PANI–AMB samples, XPS measurements were carried out. Fig. 15a shows the wide-scan XPS spectra. Comparing the wide-scan spectra before and after the adsorption of Pd(II), Pd 3d bands were clearly observed in the spectra after the adsorption of Pd(II), indicating that palladium ions were successfully adsorbed on PANI–AMB.

For the Pd-adsorbed PANI–AMB sample, the best fit for the Pd 3d spectra (Fig. 15b) was obtained with three doublets (Pd $3d_{5/2}$–$3d_{3/2}$), with a fixed doublet separation (DS). Pd $3d_{5/2}$ was observed at 335.4 eV (DS = 5.2 eV) and 337.8 eV (DS = 5.2 eV), corresponding to Pd(0) and Pd(II) in the Pd–Cl bond, respectively. The Pd $3d_{5/2}$ peak at BE = 339.2 eV (DS = 5.2 eV) can be attributed to either the Pd–N or Pd–O bond.[54]

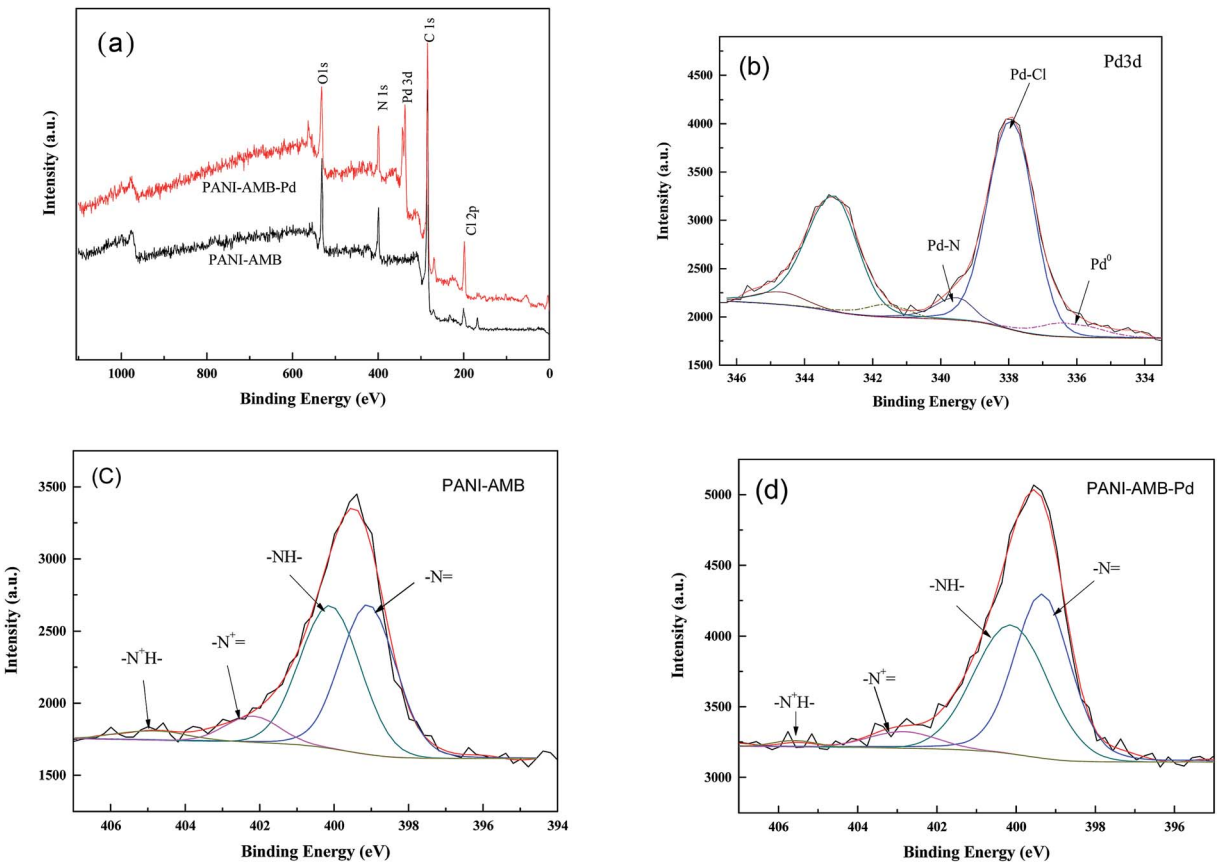

Fig. 15 The wide XPS spectra (a), palladium 3d XPS spectrum of PANI–AMB-Pd sample (b), nitrogen 1s XPS spectrum of PANI–AMB (c), nitrogen 1s XPS spectrum of PANI–AMB-Pd (d).

Fig. 15c shows the nitrogen 1s XPS spectrum of the PANI–AMB–Pd sample. The N 1s peak was resolved into four components, corresponding to imine nitrogen atoms (–N═), amine nitrogen atoms (–NH–), and two types of charged nitrogen atoms (–N^+═ and –N^+H–), respectively (Fig. 15c). The binding energy (BE) components were observed at 399.08, 400.10, 402.19, and 404.90 eV, corresponding to –N═, –NH–, –N^+═, and –N^+H–, respectively.[25] After the adsorption of palladium, the BE values for nitrogen 1s were shifted to 399.34, 400.12, 402.85, and 405.59 eV, respectively, showing a slight increase compared to the sample before the adsorption of palladium (Fig. 15d). Pd(II) can coordinate with N atoms, leading to the formation of Pd–N. The results obtained from XPS analysis clearly confirmed the formation of coordination bonds between Pd(II) and–NH–/–N═/–COOH/–OCH_3 and the reduction of Pd(II) to Pd(0) by the PANI–AMB copolymers. Thus, the XPS results supported the co-existence of chelation and redox sorption processes.

Based on the above results, a probable mechanism for the two-step adsorption on the PANI–AMB copolymer has been proposed in Scheme 2. First, according to the HSAB theory, palladium ions tend to chelate with N and O atoms. Therefore, –NH–, –OCH_3, and –COOH groups exhibit a good chelation ability with palladium ions, and the chelate between PANI–AMB and Pd(II) is formed on the copolymer surface (Scheme 2a). With the progress of sorption, Pd(II) is reduced by –NH and –NH^+═ groups to Pd(0), while benzenoid rings are oxidized into quinoid rings (Scheme 2b). The sorption mechanism can be further confirmed by measuring the variation in pH of the palladium ion solution with sorption time (Fig. 16).

Accompanying the sorption of Pd(II), H^+ was released from the copolymer chains, resulting in lower pH of the Pd(II) solution after sorption. This result is in good agreement with the mechanism proposed in Scheme 2. In addition, protonated –NH^+═ groups can also adsorb $PdCl_4^{2-}$ through electrostatic attractions between the anions and cations. Therefore, palladium ions are adsorbed on the PANI–AMB copolymer *via* a combination of three adsorption mechanisms: chelation sorption, redox adsorption, and ionic association. Chelation sorption is the dominant sorption mechanism among these three.

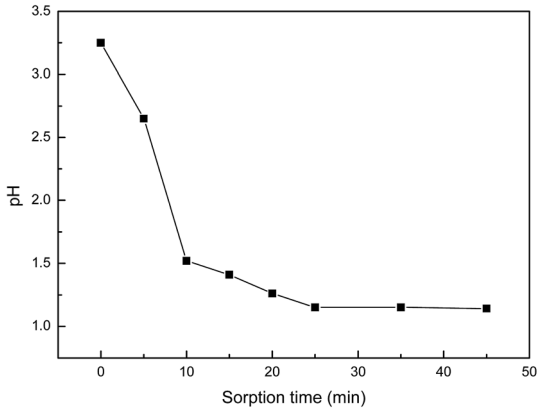

Fig. 16 Variation of pH value with sorption time.

3.8 Recovery of palladium and regeneration of PANI–AMB

The proposed method was applied for the adsorption and separation of palladium from the leaching liquor of spent automotive catalysts. Automotive catalysts were treated with smelting enrichment-wet separation process,[55] in which Pd, Pt, and Rh were captured with base metals. After zinc powder

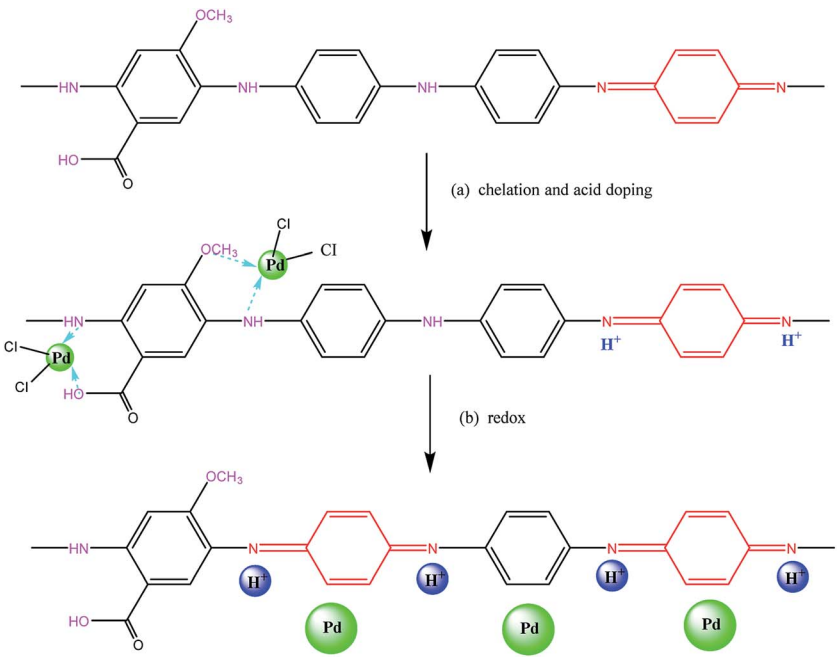

Scheme 2 The possible adsorption reactive mechanism of PANI–AMB copolymer for Pd(II): (a) surface chelate formation, (b) oxidation–reduction reactions.

replacement, the mixed metals are dissolved by acid, the final solution containing Pd, Pt, Rh, Fe, Ni Zn, Al, Cu, and Pb. P204 was used to extract base metals according to a previously reported study.[56] The compositions of the final leach liquor and percentage extractions of P204 are shown in Table 7.

Almost all base metals (>98.0%) were removed by P204, while the majority of Pd(II), Pt(IV), and Rh(III) metals remained in the solution (Table 7). The residual solution containing Pd, Pt, and Rh was evaporated to near dryness, and then the solution was diluted to a known volume with 0.1 mol L^{-1} HCl. Palladium was effectively adsorbed on the PANI–AMB copolymer in 0.1 mol L^{-1} HCl. The Pd(II)-adsorbed PANI–AMB was easily eluted by 0.5 mol L^{-1} thiourea in an HCl (1 mol L^{-1}) solution at room temperature (298 ± 1 K). The results of the selective Pd adsorption from leaching liquor of spent automotive catalysts with PANI–AMB are shown in Table 8.

Based on the experimental data in Table 8, the separation factors[57,58] $\beta_{Pd/Pt}$ and $\beta_{Pd/Rh}$ were found to be 4.3×10^3 and 5.3×10^3, respectively. More than 99.0% of Pd(II) was effectively adsorbed on the PANI–AMB copolymer in the presence of Pt(IV) and Rh(III), while only 3.2% of Pt(IV) and 2.6% of Rh(III) were adsorbed on the PANI–AMB copolymer, respectively. The elution rate of Pd(II)-loaded PANI–AMB copolymer was 98.5%, which indicates fairly good performance for the Pd(II) removal. Furthermore, the PANI–AMB copolymers were easily regenerated by treatment with a 0.1 mol L^{-1} HCl solution after elution by acidic thiourea.

To evaluate the regeneration ability of the copolymer, the maximum adsorption capacities of six adsorption–desorption cycles in single Pd(II) solutions are tested. The results are shown in Fig. 17a. Adsorption and separation of palladium from leaching liquor of spent automotive catalysts with PANI–AMB was also performed. The corresponding recovery rates for six adsorption–desorption cycles are presented in Fig. 17b.

Table 7 Composition of the leaching liquor of automotive catalysts and percentage extractions of ingredients with P204

Ions	Leaching liquor (mg L^{-1})	Residual concentration (mg L^{-1})	Percentage extraction (%)
Pd	275.8	273.6	0.80
Pt	247.2	246.1	0.44
Rh	80.5	79.6	1.1
Fe	226.5	2.3	99.0
Cu	198.6	2.9	98.5
Ni	161.8	1.5	99.1
Al	102.7	1.1	98.9
Pb	87.6	1.5	98.3
Zn	132.6	2.5	98.1

Table 8 Adsorption and separation of palladium from leaching liquor of spent automotive catalysts with PANI–AMB

Metal ion	Pd(II)	Pt(IV)	Rh(III)
Initial concentration (mg L^{-1})	273.6	246.1	79.6
Adsorption rate (%)	99.3	3.2	2.6
Separation factor ($\beta_{Pd/M} \times 10^{-3}$)		4.3	5.3
Desorption rate (%)	98.5		
Recovery rate (%)	96.9		

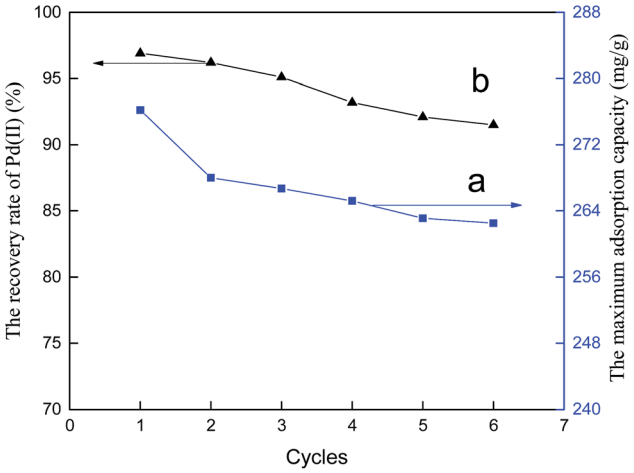

Fig. 17 The adsorption behavior of the regenerated PANI–AMB copolymers.

It can be seen from Fig. 17a that the maximum loss in the adsorption capacity after conducting six adsorption–desorption cycles did not exceed 5%. Hence, the PANI–AMB adsorbent exhibits excellent reusability in single Pd(II) solutions. In addition, the experiment found that the desorption rates for all six cycles were higher than 99.0%. In contrast, the recovery rates of Pd(II) for all six cycles were over 91.5% in the leaching liquor of spent automotive catalysts(Fig. 17b). According to the above results, the PANI–AMB adsorbent showed efficient adsorption and separation of palladium from the leaching liquor of spent automotive catalysts containing Pd(II), Pt(IV), and Rh(III), as well as good stability and reusability.

4. Conclusions

In this study, a new method for the adsorption and separation of palladium using PANI–AMB copolymers is reported. The PANI–AMB copolymers exhibited higher adsorption capacity for Pd compared to a majority of previously reported adsorbents. The optimum HCl concentration for the adsorption of Pd(II) on the PANI–AMB copolymer was determined to be 0.1 mol L^{-1}. The Langmuir isotherm model showed better fitting for the equilibrium adsorption data than the Freundlich model. The pseudo second-order equation exhibited the best correlation for the adsorption of Pd(II) on PANI–AMB copolymer. More than one mechanism was involved in the adsorption of Pd(II) on PANI–AMB copolymer. Chelation sorption was the dominant adsorption mechanism as the N and O atoms from –NH–, $–OCH_3$ and –COOH groups on the sorbent exhibited a strong chelating ability for Pd(II) and formed stable Pd chelates. In addition, redox adsorption also played an important role during adsorption. The benzenoid rings of the PANI–AMB copolymer

chains were oxidized into quinoid rings during sorption, accompanied by the reduction of Pd(II) ion to Pd metal. Thermodynamic parameters of $\Delta G < 0$ and $\Delta H > 0$ indicated that the adsorption of palladium is spontaneous and endothermic. Batch adsorption experiments indicated that the PANI–AMB copolymer exhibits excellent adsorption capacity, facile regeneration, cost-effectiveness, high selectivity, and good stability. The results obtained from this study indicate that this new PANI–AMB adsorbent can be used for the efficient separation of Pd(II) from the leaching liquor of spent automotive catalysts.

Conflicts of interest

There are no conflicts to declare.

Acknowledgements

The authors gratefully acknowledge financial support from National Natural Science Foundation of China (51264038, 51464044), National Key Basic Research Program of China (2014CB643406), Free exploration fund for academician (2016HA010, 2017 HA010) and the Natural Science Foundation of Yunnan Province (2015FB107).

References

1 M. Rajiv Gandhi, M. Yamada, Y. Kondo, A. Shibayama and F. Hamada, *J. Ind. Eng. Chem.*, 2015, **30**, 20–28.
2 J. Chen and K. Huang, *Hydrometallurgy*, 2006, **82**, 164–171.
3 A. N. Nikoloski, K.-L. Ang and D. Li, *Hydrometallurgy*, 2015, **152**, 20–32.
4 T. H. Nguyen, C. H. Sonu and M. S. Lee, *J. Ind. Eng. Chem.*, 2015, **32**, 238–245.
5 W. Wei, C.-W. Cho, S. Kim, M.-H. Song, J. K. Bediako and Y.-S. Yun, *J. Mol. Liq.*, 2016, **216**, 18–24.
6 N. F. M. Noah, N. Othman and N. Jusoh, *J. Taiwan Inst. Chem. Eng.*, 2016, **64**, 134–141.
7 P. Ramakul, Y. Yanachawakul, N. Leepipatpiboon and N. Sunsandee, *Chem. Eng. J.*, 2012, **193–194**, 102–111.
8 M. R. Awual, M. A. Khaleque, Y. Ratna and H. Znad, *J. Ind. Eng. Chem.*, 2015, **21**, 405–413.
9 C. A. Snyders, S. M. Bradshaw, G. Akdogan and J. J. Eksteen, *Hydrometallurgy*, 2014, **149**, 132–142.
10 S. Sharma, M. Barathi and N. Rajesh, *Chem. Eng. J.*, 2015, **259**, 457–466.
11 N. Das, *Hydrometallurgy*, 2010, **103**, 180–189.
12 A. Sari, D. Mendil, M. Tuzen and M. Soylak, *J. Hazard. Mater.*, 2009, **162**, 874–879.
13 M. R. Awual, M. M. Hasan and H. Znad, *Chem. Eng. J.*, 2015, **259**, 611–619.
14 Q. F. Lü, J. Y. Zhang and Z. W. He, *Chem.–Eur. J.*, 2012, **18**, 16571–16579.
15 Q. F. Lü, J. J. Luo, T.-T. Lin and Y. Z. Zhang, *ACS Sustainable Chem. Eng.*, 2014, **2**, 465–471.
16 Z. W. He, Q. F. Lu and J. Y. Zhang, *ACS Appl. Mater. Interfaces*, 2012, **4**, 369–374.
17 X. G. Li, H. Feng and M. R. Huang, *Chem.–Eur. J.*, 2010, **16**, 10113–10123.
18 H. Cui, Y. Qian, Q. Li, Q. Zhang and J. Zhai, *Chem. Eng. J.*, 2012, **211–212**, 216–223.
19 R. Li, L. Liu and F. Yang, *Chem. Eng. J.*, 2013, **229**, 460–468.
20 Y. Zhang, Q. Li, L. Sun, R. Tang and J. Zhai, *J. Hazard. Mater.*, 2010, **175**, 404–409.
21 Z. W. He, L. H. He, J. Yang and Q. F. Lü, *Ind. Eng. Chem. Res.*, 2013, **52**, 4103–4108.
22 J. Yang, J. X. Wu, Q. F. Lü and T. T. Lin, *ACS Sustainable Chem. Eng.*, 2014, **2**, 1203–1211.
23 J. J. Luo and Q. F. Lü, *Polym. Compos.*, 2015, **36**, 1546–1556.
24 J. Wang, K. Zhang and L. Zhao, *Chem. Eng. J.*, 2014, **239**, 123–131.
25 B. Qiu, C. Xu, D. Sun, Q. Wang, H. Gu, X. Zhang, B. L. Weeks, J. Hopper, T. C. Ho, Z. Guo and S. Wei, *Appl. Surf. Sci.*, 2015, **334**, 7–14.
26 J. Wang, X. Han, Y. Ji and H. Ma, *Desalin. Water Treat.*, 2014, **56**, 356–365.
27 Y. Kong, J. Wei, Z. Wang, T. Sun, C. Yao and Z. Chen, *J. Appl. Polym. Sci.*, 2011, **122**, 2054–2059.
28 X. G. Li, H. Feng and M. R. Huang, *Chem.–Eur. J.*, 2009, **15**, 4573–4581.
29 B. L. Rivas and C. O. Sánchez, *J. Appl. Polym. Sci.*, 2003, **89**, 2641–2648.
30 F. Cataldo, *Eur. Polym. J.*, 1996, **32**, 43–50.
31 X. G. Li, M. R. Huang and W. Duan, *Chem. Rev.*, 2002, **102**, 2925–3030.
32 Q. F. Lü, Z. W. He, J. Y. Zhang and Q. Lin, *J. Anal. Appl. Pyrolysis*, 2011, **92**, 152–157.
33 A. Uheida, M. Iglesias, C. Fontàs, M. Hidalgo, V. Salvadó, Y. Zhang and M. Muhammed, *J. Colloid Interface Sci.*, 2006, **301**, 402–408.
34 J. Wang, B. Deng, H. Chen, X. Wang and J. Zheng, *Environ. Sci. Technol.*, 2009, **43**, 5223–5228.
35 T. H. Nguyen, C. H. Sonu and M. S. Lee, *Hydrometallurgy*, 2016, **164**, 71–77.
36 P. P. Sun, J. Y. Lee and M. S. Lee, *Mater. Trans.*, 2011, **11**, 2071–2076.
37 T. H. Nguyen, C. H. Sonu and M. S. Lee, *J. Ind. Eng. Chem.*, 2016, **36**, 245–250.
38 F. L. Bernardis, R. A. Grant and D. C. Sherrington, *React. Funct. Polym.*, 2005, **65**, 205–217.
39 M. H. Chen, S. J. Wu, Z. J. Huang, J. Chen and M. J. Chen, *J. Chem. Technol. Biotechnol.*, 2017, **92**, 1699–1709.
40 Y. Liu, Z. J. Huang, J. F. Li and J. Chen, *J. Chil. Chem. Soc.*, 2016, **61**, 2864–2869.
41 M. R. Awual and M. M. Hasan, *J. Ind. Eng. Chem.*, 2015, **21**, 507–515.
42 Q. Ricoux, V. Bocokić, J. P. Méricq, D. Bouyer, S. V. Zutphen and C. Faur, *Chem. Eng. J.*, 2015, **264**, 772–779.
43 M. Can, E. Bulut and M. Özacar, *Chem. Eng. J.*, 2015, **275**, 322–330.
44 S. Sharma and N. Rajesh, *Chem. Eng. J.*, 2016, **283**, 999–1008.
45 S. Wang, T. Vincent, J.-C. Roux, C. Faur and E. Guibal, *Chem. Eng. J.*, 2017, **313**, 567–579.
46 S. Sharma and N. Rajesh, *Chem. Eng. J.*, 2014, **241**, 112–121.

47 O. E. Fayemi, A. S. Ogunlaja, P. F. M. Kempgens, E. Antunes, N. Torto, T. Nyokong and Z. R. Tshentu, *Miner. Eng.*, 2013, **53**, 256–265.
48 Y. Guo, H. Guo, Y. Wang, L. Liu and W. Chen, *RSC Adv.*, 2014, **4**, 14048–14054.
49 Q. Huang, X. Lin, L. Xiong, C. Huang, H. Zhang, M. Luo, L. Tian and X. Chen, *RSC Adv.*, 2017, **7**, 23896–23906.
50 A. Maleki, B. Hayati, M. Naghizadeh and S. W. Joo, *J. Ind. Eng. Chem.*, 2015, **28**, 211–216.
51 X. E. Shen, X. Q. Shan, D. M. Dong, X. Y. Hua and G. Owens, *J. Colloid Interface Sci.*, 2009, **330**, 1–8.
52 A. Drelinkiewicz, M. Hasik and M. Choczyński, *Mater. Res. Bull.*, 1998, **33**, 739–762.
53 R. Jamal, T. Abdiryim, Y. Ding and I. Nurulla, *J. Polym. Res.*, 2007, **15**, 75–82.
54 M. Hasik, A. Bernasik, A. Drelinkiewicz, K. Kowalski, E. Wenda and J. Camra, *Surf. Sci.*, 2002, **507**, 916–921.
55 F. N. Gan, Extracting noble metal from spent automotive catalyst with smelting enrichment-wet separation process, China patent, 201210060308.6, 2012.
56 L. Pan and Z. D. Zhang, *Miner. Eng.*, 2009, **22**, 1271–1276.
57 X. Chen, K. F. Lam, S. F. Mak and K. L. Yeung, *J. Hazard. Mater.*, 2011, **186**, 902–910.
58 A. Cieszynska and M. Wisniewski, *Sep. Purif. Technol.*, 2011, **80**, 385–389.